Antigen delivery by filamentous bacteriophage fd displaying an anti-DEC-205 single-chain variable fragment confers adjuvanticity by triggering a TLR9-mediated immune response

Rossella Sartorius[1], Luciana D'Apice[1], Maria Trovato[1], Fausta Cuccaro[1], Valerio Costa[2], Maria Giovanna De Leo[3], Vincenzo Manuel Marzullo[1,3], Carmelo Biondo[4], Sabato D'Auria[1,5], Maria Antonietta De Matteis[3], Alfredo Ciccodicola[2,6] & Piergiuseppe De Berardinis[1,*]

Abstract

Filamentous bacteriophage fd particles delivering antigenic determinants via DEC-205 (fdsc-αDEC) represent a powerful delivery system that induces CD8^{+} T-cell responses even when administered in the absence of adjuvants or maturation stimuli for dendritic cells. In order to investigate the mechanisms of this activity, RNA-Sequencing of fd-pulsed dendritic cells was performed. A significant differential expression of genes involved in innate immunity, co-stimulation and cytokine production was observed. In agreement with these findings, we demonstrate that induction of proinflammatory cytokines and type I interferon by fdsc-αDEC was MYD88 mediated and TLR9 dependent. We also found that fdsc-αDEC is delivered into LAMP-1-positive compartments and co-localizes with TLR9. Thus, phage particles containing a single-strand DNA genome rich in CpG motifs delivered via DEC-205 are able to intercept and trigger the active TLR9 innate immune receptor into late endosome/lysosomes and to enhance the immunogenicity of the displayed antigenic determinants. These findings make fd bacteriophage a valuable tool for immunization without administering exogenous adjuvants.

Introduction

DEC-205 has been classified as a type I C-type lectin receptor on the basis of sequence alignments (East & Isacke, 2002). It has a N-terminal cysteine-rich domain, a fibronectin type II domain and 10 C-type lectin domains and is mainly expressed on dendritic cells (DCs) (Jiang et al, 1995; Swiggard et al, 1995). It is not known which carbohydrate is recognized by DEC-205, and it has been proposed that it may function as a promiscuous antigen receptor (Jiang et al, 1995; Mahnke et al, 2000). More recently, it has been reported that DEC-205 is a cell surface receptor for CpG oligonucleotides (Lahoud et al, 2012). DEC-205 has an internalization sequence in its cytoplasmic tail and thus has endocytic capacity. It recycles through late endosomal/lysosomal compartments (Mahnke et al, 2000) facilitating the presentation of antigens targeted to DCs with antigen-bearing monoclonal antibodies in the presence of strong adjuvants such as CpG (Mahnke et al, 2005), polyinosinic-polycytidylic acid (Poly I:C) (Trumpfheller et al, 2008) or anti-CD40 antibody (Bonifaz et al, 2004). Based on these properties, the use of antigen-conjugated anti-DEC monoclonal antibody (mAb) together with adjuvant administration has been proposed for targeted vaccination strategies (Van Broekhoven et al, 2004). However, signals for DC activation are not induced by anti-DEC-205 antibodies, and their use in antigen delivery in the absence of exogenously added adjuvants induces tolerance (Hawiger et al, 2001; Bonifaz et al, 2002; Mahnke et al, 2003).

Given this scenario, we previously described the construction of phage particles able to deliver antigen determinants via DEC-205. We also reported that the administration of bacteriophage virions in the absence of adjuvants conferred immunogenicity to the displayed epitopes (Sartorius et al, 2011).

1 Institute of Protein Biochemistry, National Council of Research, Naples, Italy
2 Institute of Genetics and Biophysics A. Buzzati-Traverso, National Council of Research, Naples, Italy
3 Telethon Institute of Genetics and Medicine, Pozzuoli (NA), Italy
4 Department of Pediatric, Gynecological, Microbiological and Biomedical Sciences, University of Messina, Messina, Italy
5 Institute of Food Science, National Council of Research, Avellino, Italy
6 Department of Science and Technology, University Parthenope of Naples, Naples, Italy
 *Corresponding author. Tel.: +39 0816132566; E-mail: p.deberardinis@ibp.cnr.it

The system of antigen delivery by bacteriophage is based on modification of the phage display technology. The filamentous bacteriophage fd is well understood at both the structural and genetic level (Banner et al, 1981; Hunter et al, 1987; Straus et al, 2008). Bacteriophages only infect and multiply with their specific host, and currently, the therapeutic use of bacteriophages is back on the agenda as bacterial resistance to antibiotics becomes widespread (Reardon, 2014). It should be mentioned that the use of the bacteriophage ΦX174 to assess specific antibody responses in patients with immunodeficiencies has been reported for many years, and is considered a safe, well-tolerated and clinically useful method (Smith et al, 2014). In theory, the administration of filamentous bacteriophage fd in humans should be also considered safe, even if no human tests with this type of recombinant bacteriophage as a delivery system have been performed so far.

Overall, immunization with filamentous phages displaying antigenic peptides has been described as being able to elicit a protective immune response in animal models of disease (van Houten et al, 2006, 2010).

Filamentous bacteriophages are taken up and processed by the major histocompatibility complex (MHC) class I and II pathways (Gaubin et al, 2003) and are also able to induce an immune response mediated by cytotoxic T lymphocytes (De Berardinis et al, 1999, 2000; D'Apice et al, 2007; Sartorius et al, 2008). Importantly, we showed that phage particles displaying single-chain variable fragment (scFv) of an anti-DEC-205 monoclonal antibody were targeted to DCs and were able to induce maturation, even in the absence of maturation stimuli (Sartorius et al, 2011). Thus, the fd antigen delivery system combines the safety and capability to trigger a strong cellular antigen-specific immune response even in the absence of adjuvants.

In this work, taking advantage of next-generation sequencing (NGS) analysis, we dissected the transcriptome changes occurring in dendritic cells after exposure to fdsc-αDEC bacteriophage, and by observing the intracellular fate of fd virions targeting DEC-205, we provide insights into the immunogenicity of fd particles delivered to dendritic cells in the absence of exogenously added maturation stimuli.

Results

Immunogenicity of the ovalbumin (OVA) peptide OVA$_{257-264}$ delivered via DEC-205

We analyzed the ability of immature bone marrow-derived dendritic cells (BMDCs) loaded with lipopolysaccharide (LPS)-free fd particles displaying the peptide OVA$_{257-264}$ (SIINFEKL) (fdOVA) or fd particles co-displaying the peptide and the anti-DEC-205 scFv (fdOVA/sc-αDEC) to stimulate antigen-specific CD8$^+$ T cells. For comparative analysis, BMDCs were loaded with the same molar amount of OVA$_{257-264}$ peptide delivered by the anti-DEC-205 mAb (NLDC:pOVA). Carboxyfluorescein succinimidyl ester (CFSE)-labeled OVA$_{257-264}$-specific TCR transgenic T cells (CD8$^+$ MHC class I-restricted OT-I T cells) were used as responder cells in a proliferation assay. Fig 1A shows the proliferative activity of CD8$^+$ OT-I T cells after three days of co-culture with DCs that had been prepulsed with the antigenic preparations mentioned above. A higher proliferative response was induced by fdOVA/sc-αDEC particles compared to

fdOVA (non-targeted OVA$_{257-264}$ bacteriophage particles) and to NLDC:pOVA$_{257-264}$ (OVA$_{257-264}$ peptide delivered by anti-DEC mAb).

We also performed adoptive transfer experiments to compare the immune response to the OVA$_{257-264}$ peptide delivered to DCs by bacteriophages or by the anti-DEC-205 mAb. C57BL/6 mice, transferred with CFSE-labeled antigen-specific OT-I T cells, were injected with NLDC:pOVA or fd particles expressing the OVA$_{257-264}$ determinant (fdOVA or fdOVA/sc-αDEC) containing 1.6 μg of OVA$_{257-264}$. As a control, mice were also injected with 50 μg of soluble LPS-free ovalbumin protein or with NLDC:pOVA conjugate plus CpG as adjuvant. After 3 days, OVA$_{257-264}$-specific OT-I proliferation and IFN-γ production were evaluated. A strong proliferative response and IFN-γ production were found using fdOVA/sc-αDEC bacteriophage particles. The fdOVA particles (not displaying anti-DEC-205 scFv) or the NLDC:pOVA (OVA$_{257-264}$ peptide delivered in the same molar amount by NLDC145 mAb) induced a significantly lower antigen-specific OT-I CD8$^+$ T-cell proliferative response (Fig 1B) and no or weaker IFN-γ production (Fig 1C).The proliferative activity induced by the OVA$_{257-264}$ antigenic determinant delivered by anti-DEC-205 is low in comparison with a previous report describing the proliferation of OT-I T cells stimulated by an anti-DEC-205 antibody carrying ovalbumin protein (Bonifaz et al, 2004), while in agreement with this report (which showed lack of IFN-γ production using ovalbumin conjugated to an anti-DEC-205 antibody), we did not observe production of IFN-γ by OT-I T cells stimulated with anti-DEC antibody delivering the OVA$_{257-264}$ peptide (NLDC:pOVA, Fig 1B and C). When NLDC:pOVA conjugate was administered in the presence of the adjuvant CpG, a higher proliferative response as well as IFN-γ production by OT-I T cells was observed (Fig 1B and C). These data indicate that, in an experimental setting characterized by the absence of exogenously added adjuvants, the fd bacteriophage DEC-205-targeted particles confer strong immunogenicity to the displayed antigenic determinant.

We also observed that bacteriophage particles delivered via anti-DEC-205 scFv are internalized by dendritic cells more efficiently than non-targeted virions (Supplementary Fig S1). More than 60% of dendritic cells were fluorescein isothiocyanate (FITC) positive after incubation of BMDCs with FITC-conjugated bacteriophages expressing scFv anti-DEC-205 (fdsc-αDEC) for 30 min; this level of internalization is comparable to the value obtained for anti-DEC-205 monoclonal antibody internalization. By contrast, non-targeted fd wild-type bacteriophages (fdWT) were internalized less efficiently since only the 30% of DCs were FITC positive under the same conditions.

Importantly, BMDCs pulsed with fdsc-αDEC phage particles were able to produce IL-6 (Fig 1D), IL-18 (Fig 1E) and IFN-α (Fig 1F) while BMDCs pulsed with fdWT particles did not produce these cytokines (Fig 1D–F). In accordance with previous findings (Bonifaz et al, 2002), NLDC145 mAb in the absence of simultaneous administration of other stimuli did not elicit cytokine production (Fig 1D–F).

Transcriptome analysis by RNA-Sequencing

In order to understand the different activity shown by bacteriophage particles delivered via DEC-205, we analyzed the transcriptional profiles of DCs exposed to fdWT or fdsc-αDEC phage particles using RNA-Sequencing (RNA-Seq). Two technical replicates for each condition (DCs treated with fdWT and fdsc-αDEC) were performed.
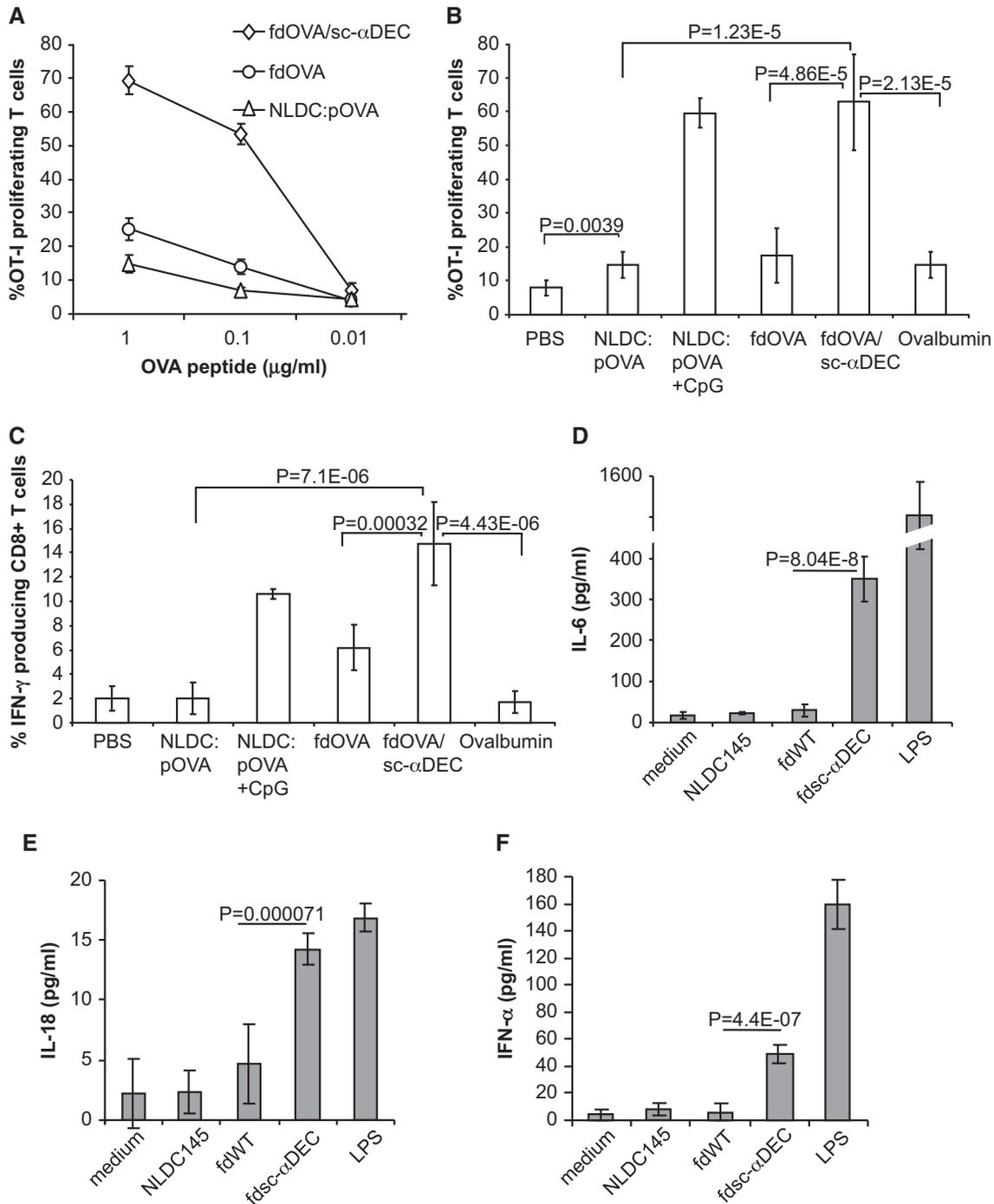
Figure 1. OVA$_{257-264}$ -specific T-cell response and cytokine production.

A   Specific CD8$^+$ T-cell (OT-I) proliferation in response to immature BMDCs incubated with fdOVA, fdOVA/sc-αDEC or OVA$_{257-264}$ peptide chemically coupled to anti-DEC-205 antibody (NLDC:pOVA). Percentage of CFSE-labeled proliferating T cells was evaluated on CD8$^+$-gated cells after 72 h of DC:T co-culture. The mean ±SD of three independent experiments is reported.

B   Proliferation of adoptively transferred OT-I T cells in C57BL/6 mice (*n* = 3/group) immunized with vehicle (PBS), NLDC:pOVA, NLDC:pOVA plus CpG, fdOVA, fdOVA/sc-αDEC or LPS-free ovalbumin protein. Percentage of CFSE-labeled proliferating OT-I T cells was evaluated after three days on Vα2$^+$ CD8$^+$-gated cells. The mean ± SD of two independent experiments is reported. Comparative analyses were performed using Student's *t*-test for unpaired samples.

C   Percentage of IFN-γ-producing CD8$^+$ splenocytes isolated from mice immunized as in (B). The mean ± SD of two independent experiments is reported. Comparative analyses were performed using Student's *t*-test for unpaired samples.

D–F   IL-6 (D), IL-18 (E) and IFN-α (F) release in supernatants of BMDCs obtained from C57BL/6 mice. Supernatants of BMDCs incubated with NLDC145 antibody, wild-type phage particles (fdWT) or scFv αDEC-205 phage particles (fdsc-αDEC) for 20 h were analyzed by ELISA for cytokine production. Unstimulated culture (medium) and LPS-treated culture were, respectively, used as negative and positive controls. Bars represent mean values ± SD. Cumulative results are shown of three independent experiments assayed in duplicate. Comparative analyses were performed using Student's *t*-test for unpaired samples.
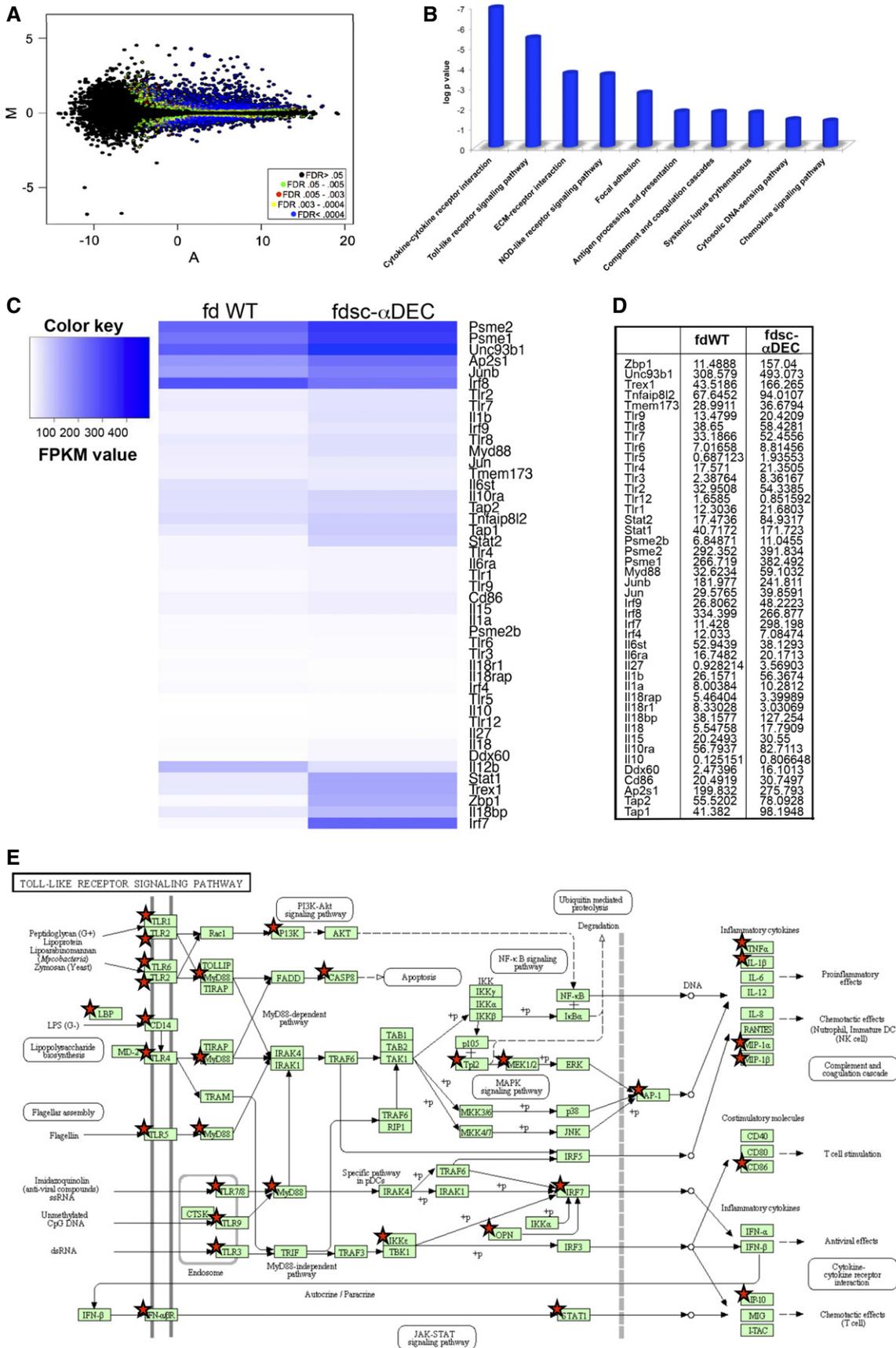
Figure 2.

Approximately 55 million reads (95% of them uniquely mapped on the reference genome) were produced for each replicate. Expression values from the biological replicates obtained for fdWT and fdsc-αDEC, computed as FPKM (fragments per kilobase of transcript and million of mapped reads), were highly correlated (Supplementary Fig S2).

Using RNA-Sequencing, we simultaneously analyzed gene expression of all genes annotated in the mouse genome. Using a threshold for gene expression levels (FPKM = 1), about 10,000 genes were expressed at significant levels in both conditions. We compared gene expression levels between the two conditions and detected approximately 4,000 genes that were differentially expressed in DCs after exposure to fdsc-αDEC compared to cells treated with fd wild-type (Fig 2A). Furthermore, to understand—in an unbiased way—whether the differentially expressed genes are significantly related to specific gene ontologies and to specific cellular pathways, we analyzed (using the Database for Annotation, Visualization and Integrated Discovery, DAVID) a stringent set of differentially expressed genes (false discovery rate (FDR) < 0.0004; see Fig 2A, blue dots). The most enriched biological pathways (KEGG database) are shown in Fig 2B. Interestingly, we observed that the exposure of DCs to fdsc-αDEC significantly up-regulated many genes that are involved in inflammatory pathways linked to innate immunity. Most relevant pathways were the cytokine–cytokine receptor and chemokine signaling pathways, the 'Toll-like receptors' (TLRs) and the 'NOD-like receptor' signaling pathways, the 'DNA sensing' and the 'antigen processing/presentation' (Fig 2B).

The heatmap in Fig 2C shows a comparison of normalized expression values of selected genes between fdWT and fdsc-αDEC-pulsed dendritic cells, with the FPKM values reported in Fig 2D. DCs treated with fdsc-αDEC mainly up-regulate genes encoding immune-related cytokines and chemokines, including *Cxcl10*, *Il1b*, *Il18* and *Il15*, and the gene encoding the co-stimulatory molecule CD86. Moreover, many interferon signaling genes such as *Ifnar2*, *Stat1*, *Stat2* and *Irf7* are differentially expressed, indicating the development of type 1 immuno-stimulatory dendritic cells (DC1).

RNA-Seq data also revealed the up-regulation of the expression of the two MHC-linked genes *Tap1* and *Tap2* that are required for the antigen-processing and presentation pathway of intracellular antigens to T cells, and of *Psme1/2* genes encoding the immune-proteasome-associated complex PA28 subunits alpha and beta. PA28β expression is low in immature DCs and strongly increases in mature DCs (Ossendorp *et al*, 2005), and more recently, it has been reported that the immunoproteasome has a major role in regulating gene transcription in maturing DCs (de Verteuil *et al*, 2014).

Our transcriptome data also show that, compared to fd wild-type, fdsc-αDEC induces the expression of genes encoding DNA sensor proteins such as STING (*Tmem173*), DAI (*Zbp1*) and TREX1 (*Trex1*) in dendritic cells. TREX1 has been described as being up-regulated by TLR ligands in murine conventional dendritic cells (Xu *et al*, 2014), and, in this context, we detected a significant up-regulation of TLR transcripts, including TLR9 which also senses DNA (Supplementary Fig S3). Moreover, we observed a significant up-regulation of transcripts encoding proteins linked to the TLR pathway (summarized in Fig 2E), such as the MYD88 adaptor molecule (Supplementary Fig S3), and proteins such as UNC93B1 involved in the trafficking of endosomal TLRs (TLR3, TLR7 and TLR9) (Supplementary Fig S3). These findings prompted us to investigate the role of TLRs after DC exposure to fdsc-αDEC.

Role of MYD88 and TLR9 in DCs targeted by phage particles displaying anti-DEC-205 scFv

The involvement of the TLR pathway in the activity induced by fdsc-αDEC particles after their internalization and/or degradation in the endolysosomal compartments was initially investigated by analyzing the production of the pro-inflammatory cytokine IL-6 in $MyD88^{-/-}$ DCs pulsed with LPS-free phage virions. As illustrated in Fig 3A, the production of IL-6 by fdsc-αDEC was totally abolished in $MyD88^{-/-}$ DCs compared to wild-type BMDCs, confirming the involvement of the TLR pathway. Since the filamentous phage particles contain a single-strand (ss) DNA rich in unmethylated CpG sequences, and since TLR9 recognizes unmethylated CpG motifs of bacterial and viral ssDNA, we next specifically investigated the role of TLR9 in the induction of cytokine production after phage uptake.

To this end, we measured IL-6 production in the supernatants of BMDCs isolated from $Tlr9^{-/-}$ mice that had been co-cultured with fdWT or fdsc-αDEC bacteriophage particles. We found that IL-6 release is severely impaired using fdsc-αDEC bacteriophages in DCs isolated from mice lacking TLR9 expression but not in DCs lacking TLR4, used as a control (Fig 3A). Interestingly, IFN-α release also appears to be linked to TLR9 signaling, since both $MyD88^{-/-}$ and $Tlr9^{-/-}$ DCs, but not $Tlr4^{-/-}$ DCs, are unable to produce IFN-α when pulsed with fdsc-αDEC bacteriophages (Fig 3B).

Furthermore, we also assessed inflammatory cytokine production in DCs isolated from immunized mice. We injected C57BL/6 mice with LPS-free fdWT or fdsc-αDEC bacteriophages. Two hours later, DCs were isolated from the spleen of immunized mice by magnetic separation, total RNA was extracted, and the expression level of IL-6 mRNA was assessed using quantitative real-time (RT) PCR. The relative gene expression was calculated using the $2^{-\Delta\Delta Ct}$ method (Livak & Schmittgen, 2001), with PBS-treated mice as calibrator and β-actin as a housekeeping gene. As shown in Fig 3C, delivering fd bacteriophage via DEC-205 scFv resulted in a strong up-regulation of IL-6 mRNA expression (up to 12-fold), while DCs isolated from mice treated with fdWT bacteriophages showed no increase.
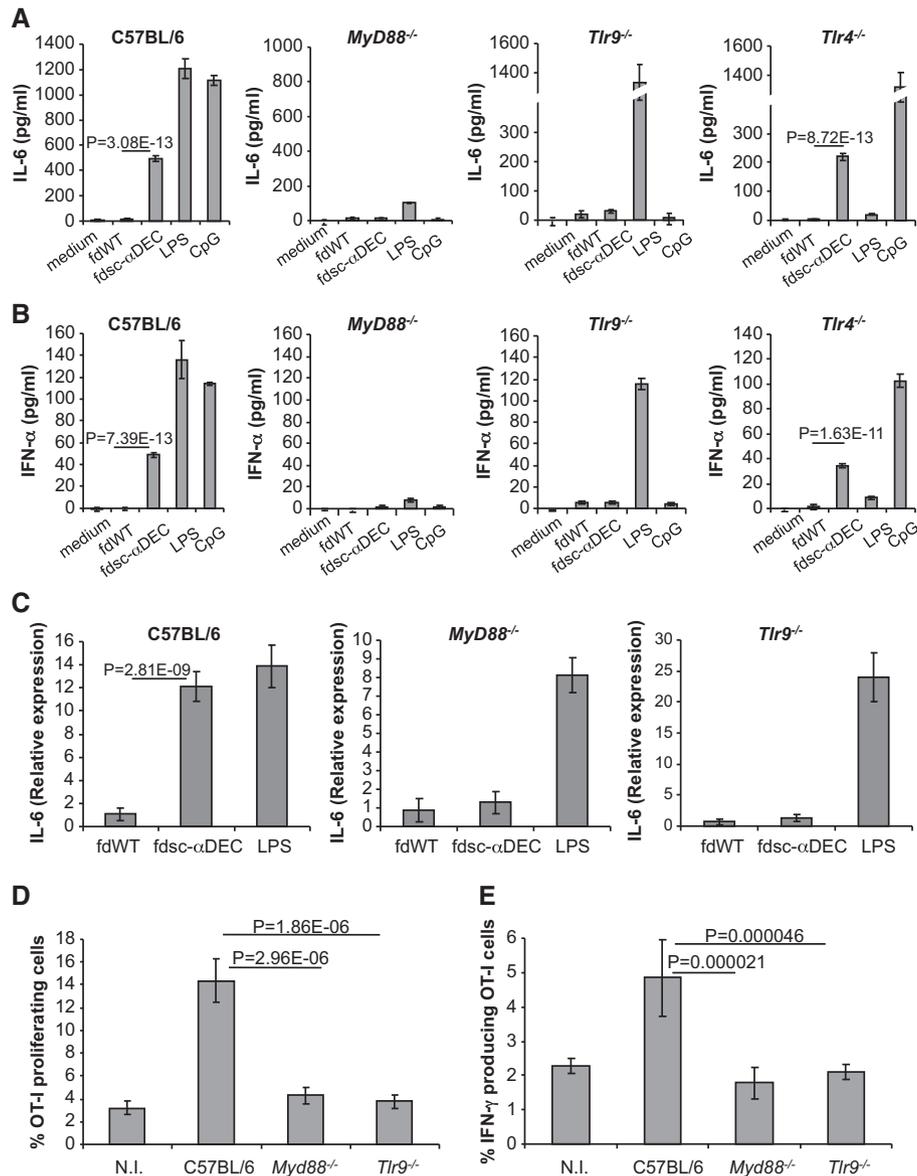
Figure 3. fdsc-αDEC induces IL-6 and IFN-α production mediated by MYD88 and TLR9.

A   IL-6 was evaluated by ELISA in supernatants of BMDCs obtained from C57BL6, MYD88, TLR9 or TLR4 KO mice and incubated for 20 h with wild-type or fdsc-αDEC phage particles. LPS or CpG-ODN were used as controls. IL-6 release from DCs derived from $MyD88^{-/-}$ mice was totally abolished and dramatically reduced in DCs derived from $Tlr9^{-/-}$ mice, but not affected in $Tlr4^{-/-}$ DCs. Bars represent mean values ± SD. Cumulative results are shown of three independent experiments assayed in duplicate. Comparative analyses were performed using Student's t-test for unpaired samples.

B   IFN-α release evaluated by ELISA in supernatants of BMDCs obtained from C57BL/6 or KO mice and incubated for 20 h with wild-type or fdsc-αDEC phage particles. LPS or CpG-ODN were used as controls. $MyD88^{-/-}$ and $Tlr9^{-/-}$ but not $Tlr4^{-/-}$ BMDCs were unable to produce IFN-α after fdsc-αDEC stimulation. Bars represent mean values ± SD. Cumulative results are shown of three independent experiments assayed in duplicate. Comparative analyses were performed using Student's t-test for unpaired samples.

C   IL-6 mRNA expression by DC cells. C57BL/6, $MyD88^{-/-}$ and $Tlr9^{-/-}$ mice were inoculated intraperitoneally with fdWT or fdsc-αDEC bacteriophages or, as a control, with LPS. Mice were sacrificed 2 h later, and purified spleen dendritic cells were analyzed for IL-6 mRNA levels by quantitative real-time PCR. Bars represent the mean fold increase ± SD. The experiments were performed three times ($n = 2$ per group). Comparative analyses were performed using Student's t-test for unpaired samples.

D   Proliferation of OT-I CD8+ T cells after 72 h of co-culture with 1×10^4 DCs isolated from C57BL/6 mice or from $MyD88^{-/-}$ or $Tlr9^{-/-}$ transgenic mice previously injected with fdOVA/sc-αDEC bacteriophage particles. The panel shows the percentage of divided, CFSE-low OT-I CD8+ T cells. As a control, the proliferation of OT-I CD8+ T cells co-cultured with DCs isolated from non-immunized (NI) C57BL/6 mice is reported. The mean ± SD of two independent experiments with $n = 3$ per group is reported. Comparative analyses were performed using Student's t-test for unpaired samples.

E   IFN-γ production by OT-I CD8+ T cells co-cultured for 12 h in the presence of 3.3×10^3 DCs isolated from C57BL/6 mice or MyD88$^{-/-}$ and Tlr9$^{-/-}$ transgenic mice injected as in (D).

Data information: The mean ± SD of two independent experiments with $n = 3$ per group is reported. Comparative analyses were performed using Student's t-test for unpaired samples.

Moreover, we measured IL-6 mRNA levels in splenic DCs isolated from $MyD88^{-/-}$ or $Tlr9^{-/-}$ mice 2 h after fdWT or fdsc-αDEC injection. As reported in Fig 3C, negligible levels of IL-6 were produced in either $MyD88^{-/-}$ or $Tlr9^{-/-}$ DCs after wild-type or fdsc-αDEC bacteriophage injection, indicating that dendritic cells targeted via anti-DEC-205 bacteriophages *in vivo*, analogously to *in vitro* treated BMDCs, are able to produce proinflammatory cytokines via TLR9/MYD88 signaling.

Finally, splenic DCs were purified by magnetic separation 18 h after the administration of the phage particles to C57BL/6, $MyD88^{-/-}$ and $Tlr9^{-/-}$ mice and co-cultivated with CFSE-labeled $OVA_{257-264}$-specific OT-I transgenic T cells. DCs isolated from C57BL/6 mice and targeted *in vivo* with fdOVA/sc-αDEC induced significant OT-I proliferation (Fig 3D) and IFN-γ production (Fig 3E), whereas DCs isolated from $MyD88^{-/-}$ and $Tlr9^{-/-}$ mice promoted neither $CD8^+$ OT-I proliferation nor IFN-γ release.

These results demonstrate that the ability of fdOVA/sc-αDEC phage particles to induce cytokines production and to confer higher immunogenicity to the displayed antigenic determinants is dependent on activation of the TLR9/MYD88 pathway.

Subcellular localization of fd particles

In order to understand how and where fdsc-αDEC intercepts TLR9, we analyzed the intracellular fate of fdsc-αDEC and of wild-type bacteriophages by dissecting the intracellular trafficking route of fd particles (delivered or not via DEC-205) in BMDCs. BMDCs incubated with tetramethylrhodamine (TRITC)-conjugated fdWT or fdsc-αDEC for 6 h were analyzed by confocal microscopy, and their endosomal compartments were mapped using early endosomal (EEA-1) or late endosomal/lysosomal (LAMP-1) markers. We observed low co-localization of fd bacteriophages particles, either wild-type or expressing anti-DEC-205, in EEA-1-positive early endosomes (< 3% of EEA-1-positive structures contain fd wild-type (Fig 4A) or fdsc-αDEC phage particles (Fig 4B)). By contrast, we found that fdsc-αDEC bacteriophages, but not fd wild-type, localized in the LAMP1-positive late endosomal/lysosomal compartments. As shown in Fig 4C and D, the display of anti-DEC-205 scFv on the phage surface markedly increases the localization of bacteriophages into late endolysosomal compartments. Co-localization analysis showed that 41.3% of LAMP-1-positive structures also contain fdsc-αDEC phage particles (Fig 4D), while fd wild-type seems to localize with only 8.9% of the LAMP-1-positive endolysosomes (Fig 4C).

These data indicate that fd particles displaying the anti-DEC-205 scFv behave like the anti-DEC-205 antibody that has been described to deliver antigens to late endosomal/lysosomal compartments (Platt *et al*, 2010).

To verify the co-localization of phage particles internalized via the DEC-205 receptor with TLR9 in dendritic cells, we expressed recombinant TLR9 C-terminally fused to yellow fluorescent protein (YFP) in BMDCs. Using TRITC-conjugated bacteriophages and confocal microscopy, we were able to assess the co-localization of phage particles internalized by DCs with the TLR9-YFP. We found that fdsc-αDEC particles, which are able to activate DCs, induce a high number of TLR9-positive structures compared to cells incubated with fd wild-type particles (Fig 5A and C, left panels). Moreover, the majority (82.3%) of the fdsc-αDEC virions co-localized with TLR9

(Fig 5C and D) compared to only 4.6% co-localization of the fd wild-type bacteriophages (Fig 5A and B).

These data of co-localization indirectly suggest that phage particles, containing a single-strand DNA genome rich in CpG motifs, when delivered via DEC-205, are able to intercept and trigger the active TLR9 innate immune receptor into the late endolysosomal compartments, and thus to enhance the immunogenicity of the displayed antigenic determinants.

Discussion

The use of *ex vivo* generated DCs pulsed with tumor antigens represents a promising immunotherapeutic option which is the object of ongoing clinical trials (Palucka & Banchereau, 2012). However, this type of vaccination is expensive and not easy to perform. A more promising approach could be the direct *in vivo* targeting of dendritic cells by coupling antigens to antibodies able to recognize receptors that are specifically expressed by DCs. In this context, it has been described that antigen-conjugated antibodies targeting C-type lectin receptors such as DEC-205 that are expressed by DCs efficiently induce antigen-specific T-cell responses (Bonifaz *et al*, 2004). However, in the case of DEC-205, this delivery is efficient only if associated with the administration of maturation stimuli for DCs, such as anti-CD40 or Poly I:C, and it is known that administration of these adjuvants may have side effects (Cornell *et al*, 1976; Levine & Levy, 1978; Cairing *et al*, 2005). To bypass this constraint, we reported that antigen-displaying filamentous bacteriophages targeting DEC-205 induce strong and protective antigen-specific T-cell responses (Sartorius *et al*, 2011). These data indicate that vaccination with phage targeted to DEC-205 does not need addition of exogenous adjuvants and that scFv anti-DEC-205 phage particles have per se adjuvant properties, being able to induce the production of pro-inflammatory cytokines and co-stimulatory molecules in DCs and to induce DC maturation (Sartorius *et al*, 2011). It is known that antigen presentation and co-stimulation provided by DCs to T cells as well as cytokines secreted by DCs determine T-cell activation. The conversion of DCs from tolerogenic to immunogenic (e.g., during infectious diseases) is thought to depend on their capacity to sense pathogen components and to produce cytokines. It is also known that cytokine gene transcription in DCs depends on the activation of transcription factors such NF-kB, Ap-1 or IRF induced by pattern recognition receptor molecules (PRR) such as the Toll-like receptors and C-type lectin receptors. However, literature data indicate that the DEC-205 type I C-type lectin receptor is not able to signal and activate transcription factors, while it is efficient in favoring the internalization of target antigens (Mahnke *et al*, 2000; Cohn *et al*, 2013). In contrast, our data show that phage particles targeting the DEC-205 receptor are able to trigger signaling in DCs. In order to investigate at the transcriptional level the mechanism of action of fdsc-αDEC particles, we used RNA-Sequencing technology on DCs after exposure to fdsc-αDEC or to wild-type fd. This analysis revealed that phages delivered via DEC-205 are able to significantly induce the expression of relevant gene pathways involved in DC activation and in the induction of efficient Th1-mediated immune responses. Here, we also describe that the activity of fdsc-αDEC particles is dependent on the recruitment of the adaptor
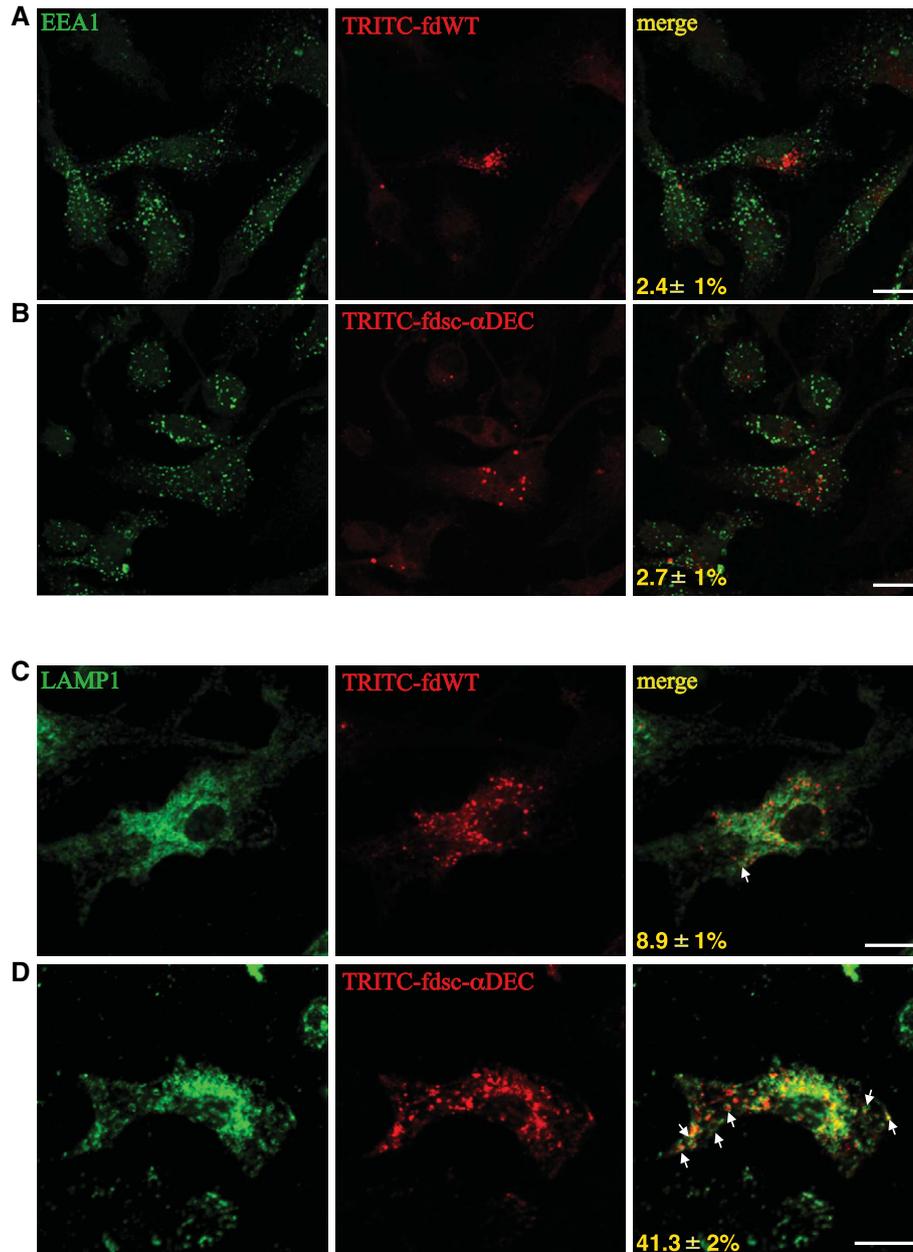
Figure 4.   Confocal microscopy analysis of BMDCs after phage uptake.

A–D   BMDCs were incubated with TRITC-conjugated fdWT (A, C) or fdsc-αDEC bacteriophages (B, D) for 6 h. Cells were then fixed, permeabilized, immunostained with anti-EEA-1 (A, B) or anti-LAMP-1 (C, D) (green) antibody and analyzed by confocal microscopy. Representative images are shown. Numbers at the bottom of the right panels indicate the percentage of EEA-1 (A, B) or LAMP-1 (C, D) bacteriophage co-localization (mean values ± SD, $N = 2$, $n = 100$). Scale bars, 10 mm. White arrows indicate LAMP-1-positive structures that also are positive or contain fdsc-αDEC or fdWT bacteriophages.

molecule MYD88. MYD88 is essential for the downstream signaling of various TLRs such as TLR9 (Häcker *et al*, 2000), and our data also demonstrate the role of TLR9 in the functional activity of DEC-205-targeted phage virions. TLR9 senses unmethylated single-stranded DNA with CpG motifs derived from bacteria and viruses (Hemmi *et al*, 2000; Mason *et al*, 2005), and phage virions contain a single-stranded genome rich in CpG motifs.

Interestingly, the RNA-Seq data indicate that phage particles addressed to late endosomes by DEC-205 are also able to up-regulate the transcription factor IRF7, which is upstream of IFN-α production, while wild-type phage (not able to access late endosomes) does not induce IRF7 up-regulation nor the production of IFN-α by DCs. Type I IFN is generally known to be produced by plasmacytoid DCs (pDCs) and the retention of signaling complexes in early endosome in pDCs rather than in late endosomes or lysosomes in other cell subsets have been correlated with IRF7 recruitment (Honda *et al*, 2005; Blasius & Beutler, 2010). It should be emphasized that mouse pDCs do not express DEC-205
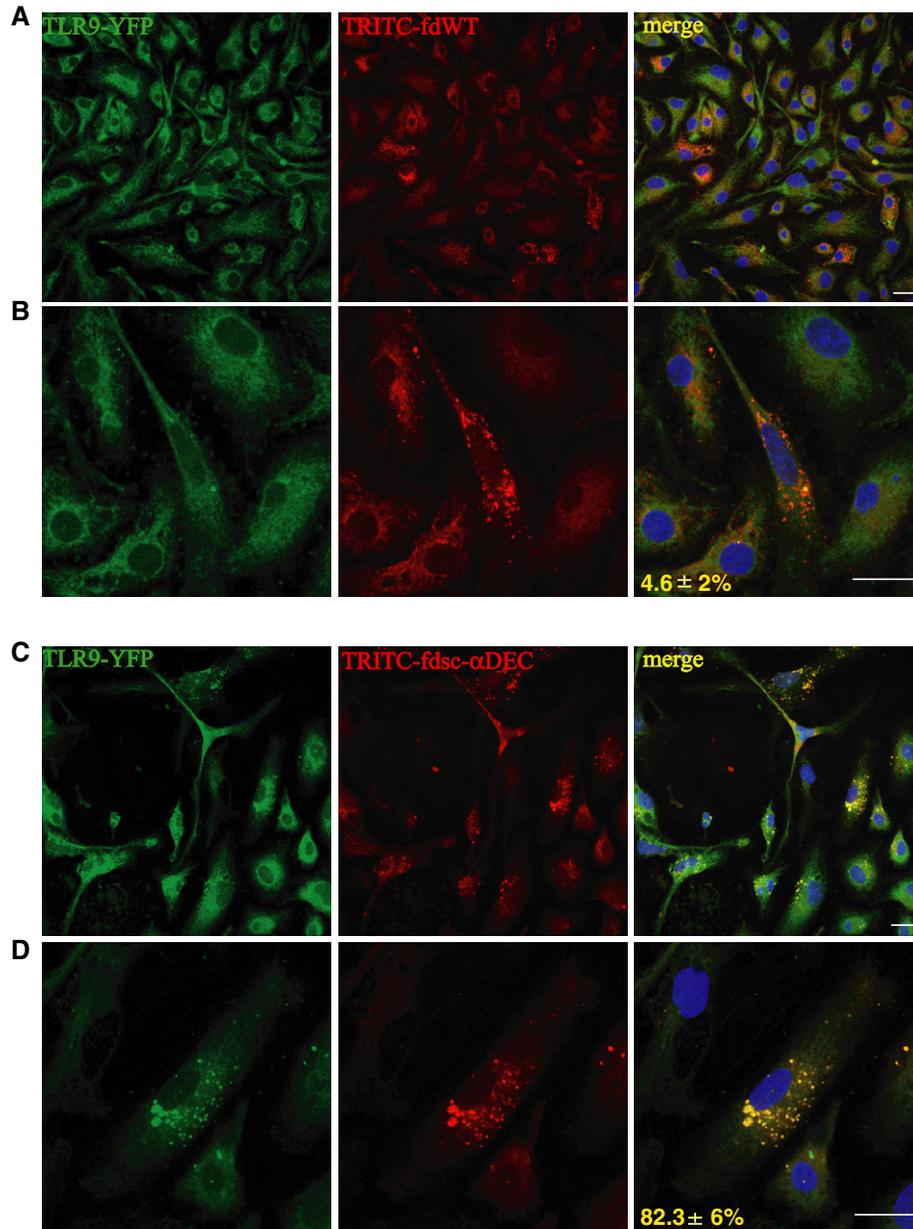
Figure 5. fdsc-αDEC localizes with TLR9 in DCs.

A–D   BMDCs from C57BL/6 mice were stably transduced with YFP-tagged TLR9. Cells grown on coverslips were then incubated with TRITC-conjugated wild-type (A, B) or fdsc-αDEC (C, D) bacteriophages for 6 h. Cells were then washed, fixed and analyzed by confocal microscopy. Nuclei were counterstained with Hoechst. (B, D) are enlargements of a single cell. Representative images are shown. Numbers at bottom of right panels indicate the percentage of TLR9 bacteriophage co-localization (mean values ± SD, $N = 2$, $n = 100$). Scale bars, 10 mm.

(Benitez-Ribas *et al*, 2011), and we have previously described the detection of IFN-α in the sera of mice immunized with fdsc-αDEC (Sartorius *et al*, 2011). Here, we provide evidence that phage particles targeted to late endosomes in BMDCs via DEC-205 are indeed able to up-regulate IRF7 and induce type I IFN production through the involvement of TLR9 and MYD88.

The majority of TLR9 is localized in the endoplasmic reticulum of DC cells before stimulation and is rapidly recruited to late endosomal/lysosomal LAMP-1-positive compartments upon activation by CpG DNA (Leifer *et al*, 2004). Only a small fraction of TLR9 constitutively moves through the cell and reaches the lysosomal compartment (Kim *et al*, 2008; Chockalingam *et al*, 2009) to provide a pool of TLR9 immediately ready to respond to endocytosed CpG DNA. This small fraction provides an initial signal, but to provide the optimal signal strength, additional TLR9 translocation from the ER to endolysosomes is required. Accordingly, we found that fdsc-αDEC, which is able to activate dendritic cells and is found in LAMP-1-positive compartments after DC internalization, is able to localize in the same compartments where TLR9 is found, while fd wild-type particles do not show a high level of co-localization with TLR9.

In order to become active, the ectodomain of TLR9 is cleaved in the endolysosome such that no full-length TLR9 is detectable in the endolysosomal compartment (Latz *et al*, 2004; Park *et al*, 2008). Importantly, only the cleaved form of TLR9 recruits MYD88 on activation (Ewald *et al*, 2008). It has been described that TLR9 signals may also lead to the activation of type I IFN and this activity requires TLR9 trafficking to a specialized compartment named the lysosome-related organelle (Sasai *et al*, 2010).

Thus, we hypothesize that phage ssDNA, targeted to DCs by DEC-205, interacts with TLR9 in late endosomes to induce the production of pro-inflammatory cytokines, and it is also delivered to lysosomal-related organelles where it signals IRF7 to induce the production of type I IFN.

The interaction between active TLR9 and phage DNA delivered via DEC-205 in endolysosomes is also supported by the fact that wild-type phage particles, which enter endolysosomal compartments only in limited amounts, are not able to elicit the production of pro-inflammatory cytokines.

Moreover, the transcriptome analysis described herein shows that DC exposure to fdsc-αDEC, but not to the wild-type bacteriophages, is able to induce up-regulation of *Unc93b1*, a gene encoding a multi-pass transmembrane protein required for TLR9 trafficking from the ER to endolysosomes. UNC93B1 remains associated with TLR9 even after Golgi processing, and the mechanism by which UNC93B1 controls the traffic of a functional TLR9 to endolysosomes has been clarified recently (Lee *et al*, 2013). In particular, these authors showed that sorting of endosomal TLR9 by UNC93B1 requires the recruitment of the adaptor protein complex (AP-2). Notably, the genes encoding two subunits of this complex (*Ap2s1* and *Ap2a2*) are up-regulated in BMDCs pulsed by fdsc-αDEC. The TLRs that recognize nucleic acids are compartmentalized to avoid unwanted activation, since discrimination between self and microbial nucleic acids is not achieved solely through recognition of distinct features but relies on differential delivery of these potential ligands to TLRs (de Jong *et al*, 2010; Chockalingam *et al*, 2012). The interaction of TLR9 with unmethylated phage ssDNA in endolysosomes may benefit from the presence of a proteinaceous coat shielding the phage ssDNA from the degradative activity of intracellular DNase. However, we can also hypothesize that phage ssDNA can escape from endosomal compartments and leak into the cytoplasm, thus activating DNA sensing molecules in the cytoplasm of fdsc-αDEC-pulsed DCs that lead to IRF7 signaling and type I IFN production.

In this context, RNA-Seq data show the up-regulation of the DNA sensing pathway and related molecules such as STING, DAI and TREX1. However, since the production of IFN-α after fdsc-αDEC stimulation is not detectable in MYD88-negative DCs, it is likely that the induction of the IRF7 transcription factor is mediated by TLR9, rather than by the above-mentioned DNA sensing molecules.

Overall, we have shown that fdsc-αDEC phage particles traffic to endolysosomal compartments and co-localize with TLR9. In contrast, phage particles not displaying DEC-205 do not reach endolysosomal compartments and do not co-localize with TLR9. Phage delivered to the endolysosomes via DEC-205 is able to induce up-regulation of different gene expression pathways and to trigger signals through TLR9 and MYD88. As a consequence, the delivery

of phage single-strand DNA in endolysosomes by fdsc-αDEC bacteriophage particles induces cytokine production and DC maturation and, as we described previously (Sartorius *et al*, 2011), strong and protective immune responses toward the displayed antigens.

Future work using fd bacteriophages displaying anti-human DEC-205 scFv will define if the activity described here can be translated to human DCs. B cells and plasmacytoid dendritic cells are the primary cells in humans that express TLR9 and respond to CpG stimulation (Hemmi *et al*, 2000; Jarrossay *et al*, 2001; Girsel *et al*, 2002; Hornung *et al*, 2002). The DEC-205 receptor has been recently described to be expressed on human plasmacytoid DCs (Tel *et al*, 2011), and accumulating evidence now suggests that pDCs are efficient in cross-presentation (Hoeffel *et al*, 2007; Di Pucchio *et al*, 2008; Lui *et al*, 2009; Tel *et al*, 2013). In addition, it has recently been reported that human myeloid CD141^{+} DCs produce cytokines in response to CpG-ODN in a whole blood assay (Hémont *et al*, 2013). Thus, in the light of these findings, it would be interesting to analyze the activity of targeted bacteriophages in the human system. Furthermore, immunotherapeutic options based on targeting B cells which also express DEC-205 can be envisaged.

In summary, using mouse BMDCs, we have demonstrated that fd carrier delivered through DEC-205 combines both the functions of immunogenicity and adjuvanticity and thus can bypass the limitations of using anti-DEC-205 monoclonal antibodies and can better exploit the use of this receptor for targeted antigen delivery.

Materials and Methods

Purification of bacteriophage particles and Western blot

Wild-type, fdsc-αDEC, fdOVA and fdOVA/sc-αDEC recombinant bacteriophages were purified as described previously (Sartorius *et al*, 2011). The number of copies of pVIII displaying the OVA$_{257-264}$ peptide was estimated by N-terminal sequence analysis of the purified virions and resulted in 15–20% for each phage preparation. The expression of the scFv anti-DEC-205 in the pIII protein of the purified virions was assessed by Western blot analysis as previously described (Sartorius *et al*, 2011). Elimination of LPS was performed by extraction with Triton X-114 (Sigma-Aldrich, Milan, Italy) according to Aida & Pabst, 1990. The final particles were tested for endotoxin using the Limulus Amebocyte Lysate (LAL) Assay (QCL-1000, Lonza, Basel, Switzerland) according to the manufacturer's instructions. The endotoxin levels were < 0.05 EU/ml in all phage preparations.

Synthesis of antibody–peptide conjugates

The NLDC145 (DEC-205/CD205 ATCC® HB-290™) hybridoma cell line producing the anti-DEC-205 antibody was obtained from the American Type Culture Collection and was maintained in RPMI 1640 medium supplemented with 10% fetal bovine serum (FBS) (Invitrogen Life Technologies, Carlsbad, CA). The NLDC145 antibody was purified from cell culture supernatants using the MAbTrap kit (GE Healthcare & Life Sciences, Milan, Italy) according to the manufacturer's instructions.

Antibodies (5 mg/ml) were reacted in 50 mM potassium phosphate (pH 7.5) with a 30-fold molar excess of N-succinimidyl S-acetylthioacetate (SATA, Thermo Fisher Scientific, Rockford, IL) for 4–6 h at 20°C. Unreacted cross-linking reagents (SATA) were removed by size-exclusion chromatography (Sephadex G25 medium, GE Healthcare, Milan, Italy) against degassed 20 mM potassium phosphate, buffered at pH 7.0 to avoid premature deacetylation on thiols. The resulting antibody was produced with an average of 3–6 blocked thiol groups covalently bound on lysine residues. The degree of linker attachment was estimated by a spectrophotometrical method immediately before subsequent peptide coupling. Briefly, DTNB (Ellman reagent), which has little if any absorbance, reacts with -SH groups on proteins under mild alkaline conditions (pH 7–8) such that the 2-nitro-5-thiobenzoate anion results in an intense absorbance at 412 nm. Since the Ellman reagent is very sensitive to buffer ions, pH and thermochromic effects, an accurate calibration curve using standard cysteine standards was performed using the same buffer as that used for the antibody. Blocking groups were then removed with 20 mM hydroxylamine (Sigma-Aldrich) and a molar excess of $OVA_{257-264}$ peptide containing an N-terminal maleimide (PRIMM, Milan, Italy) was added to approximately 30- to 40-fold molar excess over antibody and allowed to react with the new thiol groups for 2–4 h at 20°C. Excess unreacted peptide and aggregated antibodies were removed by size-exclusion chromatography against PBS. The conjugate addition between thiols and the maleimide moiety is a routine reaction, and a good yield of coupling was confirmed by the absence of any reduced sulfhydryl group on the freshly purified bioconjugate (Ellman), so the product was used as eluted from the column.

Mice

Six- to eight-week-old female C57BL/6 and ovalbumin ($OVA_{257-264}$)-specific TCR transgenic OT-I mice were purchased from Charles River (Lecco, Italy) and were maintained under specific pathogen-free conditions at the IGB Animal House Facility at CNR, Naples. $MyD88^{-/-}$, $Tlr4^{-/-}$ and $Tlr9^{-/-}$ mice were kindly donated by the University of Messina, Messina, Italy. All mice were on C57BL/6 background. Animals were randomly assigned to treatment groups. All experiments with mice were performed in accordance with European Union Laws and guidelines. All animal studies were approved by our institutional review board, and the animal procedures (i.e., immunization, sacrifice) were performed according to rules approved by the ethics committee (permission n. 137/2006-A).

Antibodies and fluorescent dyes

Antibodies used for flow cytometry/immunofluorescence, anti-CD8-PE-Cy7 (53-6.7), anti-Vα2-TCR-PE (B20.1) and anti-IFN-γ-PE (XMG1.2), were from Biolegend, San Diego, CA. Anti CD8a-APC (53-6.7) and anti-CD11c-APC (N418) were from eBioscience, San Diego, CA. Anti-CD11c-PE-Cy7 (HL3) was from BD Biosciences. Anti-DEC-205-FITC (NLDC145) was from ACRIS Antibodies GmbH, Herford, Germany.

The rabbit polyclonal antibody anti-LAMP-1 was from Abcam, Cambridge, UK. The rabbit polyclonal antibody anti-EEA-1 was from Cell Signalling, Milan, Italy. The Alexa Fluor 488 and Hoechst were from Life Technologies, Monza, Italy.

BMDCs

Bone marrow-derived dendritic cells were produced from precursors isolated from the bone marrow of C57BL/6, $MyD88^{-/-}$, $Tlr4^{-/-}$ or $Tlr9^{-/-}$ mice by culturing them with 200 U/ml recombinant murine granulocyte/macrophage colony-stimulating factor (GM-CSF) (Peprotech, NJ, USA) in RPMI 1640 (Lonza) medium supplemented with 10% FBS, 100 U/ml penicillin, 100 mg/ml streptomycin, 1 mM sodium pyruvate and 55 mM 2-mercaptoethanol (all from GIBCO, Milan, Italy). Cells were collected at day 7 of culture and were assayed for dendritic cell phenotype by staining with the monoclonal antibodies anti-CD11c and anti-DEC-205. Staining was performed in phosphate-buffered saline (PBS) containing 0.5% bovine serum albumin (BSA) for 30 min on ice using standard protocols. Data were acquired and analyzed by a BD FACSCanto II flow-cytometer and DIVA software (Becton Dickinson, Fullerton, CA).

Antigen presentation assay

Bone marrow-derived dendritic cells were incubated overnight in the presence of fdOVA, fdOVA/sc-αDEC phage particles or NLDC:$OVA_{257-264}$ peptide conjugates (all containing from 1 to 0.01 μg/ml $OVA_{257-264}$ peptide). The day after, $CD8^+$ $OVA_{257-264}$-specific T cells were purified from the spleen of OT-I mice using the $CD8^+$ T-cell isolation kit (Miltenyi Biotec, Calderara di Reno, BO, Italy), according to the manufacturer's instructions. Purified $CD8^+$ OT-I T cells were labeled with 5 mM CFSE (Sigma-Aldrich) for 10 min at 37°C. The reaction was quenched with FBS, and cells were washed 2–3 times. DCs were washed extensively to remove free antibody or phage particles and co-cultured with CFSE-labeled OT-I $CD8^+$ T cells for 72 h at a DC:T cell ratio of 1:1. After 3 days of co-culture, the CFSE intensity of OT-I T cells was evaluated on $CD8^+$-gated cells by flow cytometry using anti-CD8 mAb and a BD FACSCanto II.

Adoptive transfer and T-cell assays

CFSE-labeled OT-I $CD8^+$ T cells (3.5×10^6) were injected intravenously into C57BL/6 recipients. Twenty-four hours later, mice were immunized subcutaneously with fdOVA, fdOVA/sc-αDEC phage particles, NLDC:pOVA or NLDC:pOVA plus 50 μg cytosine-phosphate-guanosine oligodeoxynucleotides (CpG-ODN, InvivoGen, CA, USA) in 1× PBS, all containing the same dose (1.6 μg) of $OVA_{257-264}$ peptide, or with 50 μg of soluble LPS-free ovalbumin protein (ENDOGRADE Ovalbumin, Hyglos GmbH, Germany). As a control, C57BL/6 mice were injected with vehicle alone. After 3 days, splenocytes were isolated and stained with anti-Vα2 and anti-CD8 mAbs. The CFSE fluorescence intensity of adoptively transferred OT-I cells was then evaluated by flow cytometry on $CD8^+Vα2^+$ cells as previously described (Sartorius *et al*, 2011).

IFN-γ-producing $CD8^+$ T cells were evaluated by culturing 7×10^6 spleen cells with $OVA_{257-264}$ SIINFEKL peptide (10 mg/ml) for 5 h in the presence of 10 μg/ml brefeldin A (Sigma-Aldrich). Cells were then harvested, and IFN-γ production was evaluated by intracellular staining on gated $CD8^+$ T cells using PE-conjugated anti-IFN-γ mAb and Leucoperm fixation and permeabilization kit (AbD Serotec, Oxford, UK).

Analysis of *in vitro* cytokine production

To analyze IL-6, IL-18 and IFN-α production in the supernatants, DC cultures were derived from bone marrow of C57BL/6 mice and treated for 20 h with 100 μg/ml of the LPS-purified bacteriophage fd particles or anti-DEC-205 antibody NLDC145. As a positive control, supernatant was also collected from DC cultures treated with LPS (0.1 μg/ml, Sigma-Aldrich), Poly I:C (100 μg/ml) or 1 μM CpG-ODN. BMDC cells were also obtained from $MyD88^{-/-}$, $Tlr4^{-/-}$ or $Tlr9^{-/-}$ mice and treated for 20 h with 100 μg/ml of the LPS-purified bacteriophage fd particles. As a positive control, supernatant was also collected from DC cultures treated with LPS or CpG-ODN. IL-6, IL-18 or IFN-α production was measured, according to the manufacturer's instructions, using commercially available ELISA kits: ELISAMAX IL-6 standard set (Biolegend, San Diego, CA), Mouse IL-18 ELISA kit (MBL, Nagoya Aichi, Japan) or VeriKine Mouse Interferon alpha ELISA kit (pbl interferon source, Piscataway, NJ), respectively.

IL-6 expression analysis by quantitative RT–PCR

C57BL/6, $Tlr9^{-/-}$ and $MyD88^{-/-}$ mice were injected intraperitoneally with fdOVA, fdOVAsc-αDEC (100 μg/mouse) or, as a positive control, with LPS (100 μg/mouse) and sacrificed 2 h later. As a negative control, a PBS-injected mouse group was used.

Spleen cells were recovered from each mouse by cutting the spleen into small fragments and incubating with collagenase D type II (Roche Biomedical Laboratories, Burlington, NC) solution (2 mg/ml) for 30 min at 37°C. Digestion was stopped before collection of cell suspensions. The resulting material was then passed through a 70-μm cell strainer, and the recovered cells were subjected to dendritic cell enrichment using magnetic separation with mouse Pan DC microbeads and a MACS separator (Miltenyi Biotec), according to the manufacturer's instructions.

Total RNA was isolated using Tri Reagent (Sigma-Aldrich) according to the manufacturer's instructions. The integrity and quality of RNA were assessed by denaturing agarose gel electrophoresis and by Experion (Bio-Rad, Segrate (MI), Italy). RNA quantification was assessed by spectrophotometry (NanoDrop Technologies). For each sample, 500 ng of total RNA was reverse-transcribed into complementary DNA (cDNA) using the High-Capacity cDNA Reverse Transcription Kit (Life Technologies) according to the manufacturer's protocol. cDNAs were used as template for quantitative real-time polymerase chain reaction assays. The amplification reaction mix contained 1× iTaq™ Universal SYBR® Green Supermix (Bio-Rad), 300 nM of each primer and 50 ng of cDNA (RNA equivalent) as a template. PCR conditions were 95°C for 10 min followed by 40 cycles of 95°C × 30 s, 60°C × 30 s and 72°C × 30 s. Melting curves were generated after amplification. Data were collected using the CFX Connect™ Real-Time PCR Detection System (Bio-Rad); each reaction was performed in duplicate. The relative gene expression was calculated using the $2^{-\Delta\Delta Ct}$ method (Livak & Schmittgen, 2001), using as calibrator PBS-treated mice and β-actin as a housekeeping gene. Primers were designed using Oligo 4.0-s. Sequences of the primers are as follows: *Il6*-for 5′gcctattgaaaatttcctctgg3′; *Il6*-rev 5′ggaaattggggtaggaaggac3′; *Actb*-for 5′ttctttgcagctccttcgtt3′; *Actb*-rev 5′gcacatgccggagccgtt3′.

OVA$_{257-264}$-specific immune response using *ex vivo* isolated DCs

C57BL/6, $Tlr9^{-/-}$ and $MyD88^{-/-}$ mice were injected intraperitoneally with 50 μg of fdOVAsc-αDEC 18 h before sacrifice. Dendritic cells were isolated from the spleen of immunized mice as described above.

CD8$^+$ OVA$_{257-264}$-specific T cells were isolated from OT-I mice and labeled with 5 mM CFSE. A total of 100,000 CD8$^+$ OT-I purified T cells were added to each well of 96-well flat-bottom plates containing 10,000 DCs isolated from wild-type or KO mice. Proliferation of OVA-specific T cells was determined by flow cytometry after culture at 37°C in 5% CO$_2$ for 72 h. Cells were stained with anti-Vα2 mAb before acquisition on FacsCanto II (BD Biosciences). IFN-γ release was assessed by intracellular staining of purified OT-I CD8$^+$ T cells co-cultured for 12 h in the presence of 10 μg/ml brefeldin A and 3,300 C57BL/6, $Myd88^{-/-}$ or $Tlr9^{-/-}$ splenic DCs isolated from mice treated as above. The percentage of IFN-γ-producing OT-I CD8$^+$ T cells was evaluated on CD8$^+$-gated cells by flow cytometry using an anti-IFN-γ mAb and Leucoperm fixation and permeabilization kit.

RNA-Seq library production, sequencing and data analysis

Bone marrow-derived dendritic cells were plated in the presence of 100 μg/ml of the LPS-purified bacteriophage fd wild-type or fdsc-αDEC for 20 h. Total RNA was extracted as described above. RNA quality was assessed as described in Costa *et al*, 2011. Paired-end libraries (100 × 2 bp) were prepared using the TruSeq RNA Sample Preparation Kit (Illumina), following the manufacturer's instructions. Libraries were sequenced on the Illumina HiSeq2000 NGS platform at high coverage. A total of about 220 million paired-end reads were sequenced. The quality of sequenced reads was assessed using FastQC (http://www.bioinformatics.babraham.ac.uk/projects/fastqc/). TopHat version 2.0.10 (Kim *et al*, 2013) was used to map the reads against the reference mouse genome (mm9) and the RefSeq mouse transcript annotation, with default parameters. RefSeq track was downloaded from Table Browser of UCSC (http://genome.ucsc.edu). Only uniquely mapped reads (about 95% of sequenced reads) were used for further analyses. Coverage files were produced using BEDTools. Visual inspection of reads and coverage files on UCSC Genome Browsers was used to assess the overall quality of the RNA-Seq experiment, and to inspect gene-specific features. Gene expression quantification was performed using Cufflinks (Trapnell *et al*, 2010). The high correlation score of the replicates (mean Pearson's coefficient $r = 0.95$) indicated the high reproducibility of the RNA-Seq experiment. Normalized gene expression values (FPKM) for each condition were used to identify differentially expressed genes using Cuffdiff and CummeRBund (Trapnell *et al*, 2012). Gene ontology and pathway analysis were performed using DAVID (Huang *et al*, 2009). The RNA-Sequencing data from this manuscript have been submitted to the Gene Expression Omnibus (G.E.O.) database (http://www.ncbi.nlm.nih.gov/geo/) and assigned the identifier GSE60231.

FITC and TRITC conjugation of bacteriophage particles and internalization assay

Fluorescein isothiocyanate conjugation to bacteriophage particles was performed using FITC isomer I (Sigma-Aldrich) as previously described (Sartorius *et al*, 2011). TRITC conjugation of bacteriophages

was performed using TRITC from Thermo Fisher Scientific. Briefly, TRITC was added to purified bacteriophages at 6 mg/ml, and the solution was incubated for 2 h at room temperature in the dark. The excess of TRITC was removed by dialysis against 100 mM carbonate/bicarbonate buffer, pH 9.0. The number of fluors per phage was estimated from the UV absorption spectrum of purified and conjugated filamentous phage.

For the internalization assay, BMDCs (10^6 cells per well) were incubated at 37°C with FITC-conjugated fdsc-αDEC, fdWT bacteriophage particles (100 µg/ml) or NLDC145 antibody. The cells were collected and analyzed by flow cytometry at various time intervals of incubation.

Vector construction and production of recombinant lentiviral particles

The mouse TLR9-YFP sequence was a kind gift of Prof. Alexander Dalpke, University of Heidelberg, Germany.

The TLR9-YFP sequence was digested with NheI/XhoI and introduced into the same sites of the pTY2CMV-IRES-WPRE plasmid, kindly provided by Dr. A. Cara, 'Istituto Superiore di Sanità', Italy, to produce the pTY2-TLR9-YFP plasmid.

Recombinant lentiviral particles were produced as described in Negri *et al*, 2010. Briefly, HEK293T cells (ATCC CRL 1573) were transfected with pTY2-TLR9-YFP, the packaging plasmid pCMVdR8.2 and the vesicular stomatitis virus G glycoprotein (VSV-G) envelope-expressing pMD.G plasmid. The vector-containing supernatant was clarified and concentrated by ultracentrifugation (Beckman Coulter, Fullerton, CA) on a 20% sucrose gradient. Viral pellets were resuspended in 1 × PBS, and viral titer was evaluated by cytofluorimetric analysis of YFP expression after HK293 T-cell infection.

Transduction with lentiviral vectors and Immunofluorescence

For lentiviral infection, bone marrow mononuclear cells were cultured at 50,000 cells/well in 24-well plates on glass coverslips in the presence of GM-CSF (200 U/ml) and infected with concentrated viral supernatant at MOI 5 at day 1. At day 7, the glass coverslips were collected and incubated with TRITC-conjugated phage particles for 6 h at 37°C. Cells were then washed three times in PBS, fixed in 4% paraformaldehyde (PFA) (Electron Microscopy Sciences, Hatfield, PA) for 10 min, washed three times in PBS and mounted on glass slides using Mowiol (Life Technologies). Nuclei were counterstained with Hoechst. For EEA-1 and LAMP-1 staining, BMDCs at day 7 were collected and seeded onto glass coverslips at 5×10^5 cells/well in 24 well plates. At day 8, the glass coverslips were collected and incubated with TRITC-conjugated phage particles for 6 h at 37°C. Cells were then washed three times in PBS, fixed in 4% PFA for 10 min, permeabilized in 0.05% saponin (Sigma-Aldrich) and counterstained with anti-rat Alexa Fluor-488. Following labeling, coverslips were washed three times in PBS and mounted on glass slides.

Confocal fluorescence microscopy, image processing and co-localization analysis

Immunofluorescence microscopy and quantitative image analysis were performed as described (Daniele *et al*, 2008; Vicinanza *et al*, 2011). Images were acquired on a Zeiss LSM 700 confocal laser

scanning microscope, using a 65× oil-immersion objective and Zeiss' ZEN imaging software.

The experiments were repeated twice, and representative images are shown. The level of co-localization (i.e., LAMP1-fdWT, LAMP1-fdsc-αDEC, TLR9-fdWT, TLR9-fdsc-αDEC) was calculated by acquiring confocal serial sections from about 30 cells, exported in TIFF format and processed as previously described (Daniele *et al*, 2008; Vicinanza *et al*, 2011).

Statistical analysis

Results are expressed as the mean ± SD. All data were tested with the Kolmogorov–Smirnov test for normal distribution. The statistical significance of differences between experimental groups was calculated using the unpaired two-tailed Student's *t*-test with equal variance. All exact *P*-values are indicated in each figure. Differences were considered statistically significant when *P*-values were < 0.05.

Supplementary information for this article is available online: http://embomolmed.embopress.org

The paper explained

Problem

A promising immunotherapeutic approach relies on the direct targeting of dendritic cells (DCs) by coupling antigens to antibodies able to recognize the DEC-205 receptor which is specifically expressed by DCs. However, it has been widely reported that this delivery is efficient only if associated with the administration of maturation stimuli for DCs, such as anti-CD40 or Poly I:C, and it is known that administration of these adjuvants may have side effects. In this context, we previously reported the induction of protective CD8$^+$ T-cell responses by immunizing with filamentous bacteriophage fd particles displaying an anti-DEC-205 single-chain variable fragment (fdsc-αDEC) in the absence of adjuvants or maturation stimuli for dendritic cells.

Results

In this study, we provide evidence for the fdsc-αDEC mechanism of action by showing that antigen delivery by filamentous fd bacteriophage to dendritic cells via DEC-205 in the absence of adjuvants determines the up-regulation of several gene pathways involved in the immune response such as TLR genes, co-stimulatory genes and genes coding for pro-inflammatory cytokines. In addition, we observed that the production of these cytokines was MYD88 mediated and TLR9 dependent. Finally, we demonstrated that filamentous bacteriophages containing a single-strand DNA genome rich in CpG motifs are addressed to the late endosome compartments where they co-localize with TLR9 molecules, present in these compartments in their active form. We conclude that this interaction enhances the immunogenicity of the antigenic determinants displayed on the phage scaffold.

Impact

These findings make filamentous bacteriophage fd particles a valuable tool for immunization without administering exogenous adjuvants. Bacteriophage production is economically advantageous, and all available evidence indicates that administration of different strains of bacteriophages is harmless to humans. Thus, this study may be relevant concerning the possibility to use this system in humans.

Author contributions

RS designed and performed the experiments and analyzed the data. LDA, MT and FC performed experiments of immunogenicity and cytokine production and critically reviewed the manuscript. VC performed the RNA-Seq and the bioinformatics analysis. VMM and SD performed the synthesis and validation of NLDC:OVA conjugates. MGDL performed and analyzed immunofluorescence experiments. CB provided KO mice. MADM analyzed immunofluorescence data and critically reviewed the manuscript. AC supervised the bioinformatics analysis. PDB supervised the project and wrote the manuscript.

Conflict of interest

The authors declare that they have no conflict of interest.

References

Aida Y, Pabst MJ (1990) Removal of endotoxin from protein solutions by phase separation using Triton X-114. *J Immunol Methods* 132: 191–195

Banner DW, Nave C, Marvin DA (1981) Structure of the protein and DNA in fd filamentous bacterial virus. *Nature* 289: 814–816

Benitez-Ribas TJ, Hoosemans DS, Cambi A, Adema GJ, Figdor CG, Tacken PJ, de Vries IJ (2011) DEC-205 mediates antigen uptake and presentation by both resting and activated human plasmacytoid dendritic cells. *Eur J Immunol* 41: 1014–1023

Blasius AL, Beutler B (2010) Intracellular toll-like receptors. *Immunity* 32: 305–315

Bonifaz L, Bonnyay D, Mahnke K, Rivera M, Nussenzweig MC, Steinman RM (2002) Efficient targeting of protein antigen to the dendritic cell receptor DEC-205 in the steady state leads to antigen presentation on major histocompatibility complex class I products and peripheral CD8 + T cell tolerance. *J Exp Med* 196: 1627–1638

Bonifaz LC, Bonnyay DP, Charalambous A, Darguste DI, Fujii S, Soares H, Brimnes MK, Moltedo B, Moran TM, Steinman RM (2004) In vivo targeting of antigens to maturing dendritic cells via the DEC-205 receptor improves T cell vaccination. *J Exp Med* 199: 815–824

Cairing J, Barr T, Heath AW (2005) Adjuvanticity of anti-CD40 in vaccine development. *Curr Opin Mol Ther* 7: 73–77

Chockalingam A, Brooks JC, Cameron JL, Blum LK, Leifer CA (2009) TLR9 traffics through the Golgi complex to localize to endolysosomes and respond to CpG DNA. *Immunol Cell Biol* 87: 209–217

Chockalingam A, Rose WA 2nd, Hasan M, Ju CH, Leifer CA (2012) Cutting edge: a TLR9 cytoplasmic tyrosine motif is selectively required for proinflammatory cytokine production. *J Immunol* 188: 527–530

Cohn L, Chatterjee B, Esselborn F, Smed-Sörensen A, Nakamura N, Chalouni C, Lee BC, Vandlen R, Keler T, Lauer P *et al* (2013) Antigen delivery to early endosomes eliminates the superiority of human blood BDCA3 + dendritic cells at cross presentation. *J Exp Med* 210: 1049–1063

Cornell CJ Jr, Smith KA, Cornwell GG 3rd, Burke GP, McIntyre OR (1976) Systemic effects of intravenous polyriboinosinic-polyribocytidylic acid in man. *J Natl Cancer Inst* 57: 1211–1216

Costa V, Angelini C, D'Apice L, Mutarelli M, Casamassimi A, Sommese L, Gallo MA, Aprile M, Esposito R, Leone L *et al* (2011) Massive-scale RNA-Seq analysis of non ribosomal transcriptome in human trisomy 21. *PLoS ONE* 20: e18493

Daniele T, Di Tullio G, Santoro M, Turacchio G, De Matteis MA (2008) ARAP1 regulates EGF receptor trafficking and signalling. *Traffic* 9: 2221–2235

D'Apice L, Sartorius R, Caivano A, Mascolo D, Del Pozzo G, Di Mase DS, Ricca E, Li Pira G, Manca F, Malanga D *et al* (2007) Comparative analysis of new innovative vaccine formulations based on the use of procaryotic display systems. *Vaccine* 25: 1993–2000

De Berardinis P, D'Apice L, Prisco A, Ombra MN, Barba P, Del Pozzo G, Petukhov S, Malik P, Perham RN, Guardiola J (1999) Recognition of HIV-derived B and T cell epitopes displayed on filamentous phages. *Vaccine* 17: 1434–1441

De Berardinis P, Sartorius R, Fanutti C, Perham RN, Del Pozzo G, Guardiola J (2000) Phage display of peptide epitopes from HIV-1 elicits strong cytolytic responses. *Nat Biotechnol* 18: 873–876

Di Pucchio T, Chatterjee B, Smed-Sörensen A, Clayton S, Palazzo A, Montes M, Xue Y, Mellman I, Banchereau J, Connolly JE (2008) Direct proteasome-independent cross-presentation of viral antigen by plasmacytoid dendritic cells on major histocompatibility complex class I. *Nat Immunol* 9: 551–557

East L, Isacke CM (2002) The mannose receptor family. *Biochim Biophys Acta* 1572: 364–386

Ewald SE, Lee BL, Lau L, Wickliffe KE, Shi GP, Chapman HA, Barton GM (2008) The ectodomain of Toll-like receptor 9 is cleaved to generate a functional receptor. *Nature* 456: 658–662

Gaubin M, Fanutti C, Mishal Z, Durrbach A, De Berardinis P, Sartorius R, Del Pozzo G, Guardiola J, Perham RN, Piatier-Tonneau D (2003) Processing of filamentous bacteriophages virions in antigen-presenting cells targets both HLA class I and class II peptide loading compartments. *DNA Cell Biol* 22: 11–18

Girsel M, Verthelyi D, Gursel I, Ishii KJ, Klinman DM (2002) Differential and competitive activation of human immune cells by distinct classes of CpG oligodeoxynucleotides. *J Leukoc Biol* 71: 813–820

Häcker H, Vabulas RM, Takeuchi O, Hoshino K, Akira S, Wagner H (2000) Immune cell activation by bacterial CpG-DNA through myeloid differentiation marker 88 and tumor necrosis factor receptor-associated factor (TRAF)6. *J Exp Med* 192: 595–600

Hawiger D, Inaba K, Dorsett Y, Guo M, Mahnke K, Rivera M, Ravetch JV, Steinman RM, Nussenzweig MC (2001) Dendritic cells induce peripheral T cell unresponsiveness under steady state conditions in vivo. *J Exp Med* 194: 769–780

Hemmi H, Takeuchi O, Kawai T, Kaisho T, Sato S, Sanjo H, Matsumoto M, Hoshino K, Wagner H, Takeda K *et al* (2000) A Toll-like receptor recognizes bacterial DNA. *Nature* 408: 740–745

Hémont C, Neel A, Heslan M, Braudeau C, Josien R (2013) Human blood mDC subsets exhibit distinct TLR repertoire and responsiveness. *J Leukoc Biol* 93: 599–609

Hoeffel G, Ripoche AC, Matheoud D, Nascimbeni M, Escriou N, Lebon P, Heshmati F, Guillet JG, Gannagé M, Caillat-Zucman S *et al* (2007) Antigen crosspresentation by human plasmacytoid dendritic cells. *Immunity* 27: 481–492

Honda K, Ohba Y, Yanai H, Negishi H, Mizutani T, Takaoka A, Taya C, Taniguchi T (2005) Spatiotemporal regulation of MyD88-IRF-7 signalling for robust type-I interferon induction. *Nature* 434: 1035–1040

Hornung V, Rothenfusser S, Britsch S, Krug A, Jahrsdörfer B, Giese T, Endres S, Hartmann G (2002) Quantitative expression of toll-like receptor 1-10

mRNA in cellular subsets of human peripheral blood mononuclear cells and sensitivity to CpG oligodeoxynucleotides. *J Immunol* 168: 4531−4537

van Houten NE, Henry KA, Smith GP, Scott JK (2010) Engineering filamentous phage carriers to improve focusing of antibody responses against peptides. *Vaccine* 28: 2174−2185

van Houten NE, Zwick MB, Menendez A, Scott JK (2006) Filamentous phage as an immunogenic carrier to elicit focused antibody responses against a synthetic peptide. *Vaccine* 24: 4188−4200

Huang DW, Sherman BT, Lempicki RA (2009) Systematic and integrative analysis of large gene lists using DAVID bioinformatics resources. *Nat Protoc* 4: 44−57

Hunter GJ, Rowitch DH, Perham RN (1987) Interactions between DNA and coat protein in the structure and assembly of filamentous bacteriophage fd. *Nature* 327: 252−254

Jarrossay D, Napolitani G, Colonna M, Sallusto F, Lanzavecchia A (2001) Specialization and complementarity in microbial molecule recognition by human myeloid and plasmacytoid dendritic cells. *Eur J Immunol* 31: 3388−3393

Jiang W, Swiggard WJ, Heufler C, Peng M, Mirza A, Steinman RM, Nussenzweig MC (1995) The receptor DEC-205 expressed by dendritic cells and thymic epithelial cells is involved in antigen processing. *Nature* 375: 151−155

de Jong SD, Basha G, Wilson KD, Kazem M, Cullis P, Jefferies W, Tam Y (2010) The immunostimulatory activity of unmethylated and methylated CpG oligodeoxynucleotide is dependent on their ability to colocalize with TLR9 in late endosomes. *J Immunol* 184: 6092−6102

Kim D, Pertea G, Trapnell C, Pimentel H, Kelley R, Salzberg SL (2013) TopHat2: accurate alignment of transcriptomes in the presence of insertions, deletions and gene fusions. *Genome Biol* 14: R36

Kim YM, Brinkmann MM, Paquet ME, Ploegh HL (2008) UNC93B1 delivers nucleotide-sensing toll-like receptors to endolysosomes. *Nature* 452: 234−238

Lahoud MH, Ahmet F, Zhang JG, Meuter S, Policheni AN, Kitsoulis S, Lee CN, O'Keeffe M, Sullivan LC, Brooks AG *et al* (2012) DEC-205 is a cell surface receptor for CpG oligonucleotides. *Proc Natl Acad Sci USA* 109: 16270−16275

Latz E, Schoenemeyer A, Visintin A, Fitzgerald KA, Monks BG, Knetter CF, Lien E, Nilsen NJ, Espevik T, Golenbock DT (2004) TLR9 signals after translocating from the ER to CpG DNA in the lysosome. *Nat Immunol* 5: 190−198

Lee BL, Moon JE, Shu JH, Yuan L, Newman ZR, Schekman R, Barton GM (2013) UNC93B1 mediates differential trafficking of endosomal TLRs. *Elife* 2: e00291

Leifer CA, Kennedy MN, Mazzoni A, Lee C, Kruhlak MJ, Segal DM (2004) TLR9 is localized in the endoplasmic reticulum prior to stimulation. *J Immunol* 173: 1179−1183

Levine AS, Levy HB (1978) Phase I-II trials of poly IC stabilized with poly-L-lysine. *Cancer Treat Rep* 62: 1907−1912

Livak KJ, Schmittgen TD (2001) Analysis of relative gene expression data using real-time quantitative PCR and the 2(-Delta Delta C(T) method. *Methods* 25: 402−408

Lui G, Manches O, Angel J, Molens JP (2009) Plasmacytoid dendritic cells capture and cross present viral antigens from influenza virus exposed cells. *PLoS ONE* 4: e7111

Mahnke K, Guo M, Lee S, Sepulveda H, Swain SL, Nussenzweig M, Steinman RM (2000) The dendritic cell receptor for endocytosis, DEC-205, can recycle and enhance antigen presentation via major histocompatibility complex class II-positive lysosomal compartments. *J Cell Biol* 151: 673−684

Mahnke K, Qian Y, Fondel S, Brueck J, Becker C, Enk AH (2005) Targeting of antigens to activated dendritic cells in vivo cures metastatic melanoma in mice. *Cancer Res* 65: 7007−7012

Mahnke K, Qian Y, Knop J, Enk AH (2003) Induction of CD4 + /CD25 + regulatory T cells by targeting of antigens to immature dendritic cells. *Blood* 101: 4862−4869

Mason KA, Ariga H, Neal R, Valanas D, Hunter N, Krieg AM, Whisnant JK, Milas L (2005) Targeting toll-like receptor 9 with CpG oligodeoxynucleotides enhances tumor response to fractionated radiotherapy. *Clin Cancer Res* 11: 361−369

Negri DR, Bona R, Michelini Z, Leone P, Macchia I, Klotman ME, Salvatore M, Cara A (2010) Transduction of Human Antigen-Presenting Cells with Integrase-Defective Lentiviral Vector Enables Functional Expansion of Primed Antigen-Specific CD8 + T Cells. *Hum Gene Ther* 21: 1029−1035

Ossendorp F, Fu N, Camps M, Granucci F, Gobin SJ, van den Elsen PJ, Schuurhuis D, Adema GJ, Lipford GB, Chiba T *et al* (2005) Differential expression regulation of the alpha and beta subunits of the PA28 proteasome activator in mature dendritic cells. *J Immunol* 174: 7815−7822

Palucka K, Banchereau J (2012) Cancer immunotherapy via dendritic cells. *Nat Rev Cancer* 12: 265−277

Park B, Brinkmann MM, Spooner E, Lee CC, Kim YM, Ploegh HL (2008) Proteolytic cleavage in an endolysosomal compartment is required for activation of Toll-like receptor 9. *Nat Immunol* 9: 1407−1414

Platt CD, Ma JK, Chalouni C, Ebersold M, Bou-Reslan H, Carano RA, Mellman I, Delamarre L (2010) Mature dendritic cells use endocytic receptors to capture and present antigens. *Proc Natl Acad Sci U S A* 107: 4287−4292

Reardon S (2014) Phage therapy gets revitalized. *Nature* 510: 15−16

Sartorius R, Bettua C, D'Apice L, Caivano A, Trovato M, Russo D, Zanoni I, Granucci F, Mascolo D, Barba P *et al* (2011) Vaccination with filamentous bacteriophages targeting DEC-205 induces DC maturation and potent anti-tumor T-cell responses in the absence of adjuvants. *Eur J Immunol* 41: 2573−2584

Sartorius R, Pisu P, D'Apice L, Pizzella L, Romano C, Cortese G, Giorgini A, Santoni A, Velotti F, De Berardinis P (2008) The use of filamentous bacteriophage fd to deliver MAGE-A10 or MAGE-A3 HLA-A2-restricted peptides and to induce strong antitumor CTL responses. *J Immunol* 180: 3719−3728

Sasai M, Linehan MM, Iwasaki A (2010) Bifurcation of Toll-like receptor 9 signaling by adaptor protein 3. *Science* 329: 1530−1534

Smith LL, Buckley R, Lugar P (2014) Diagnostic immunization with bacteriophage ΦX 174 in patients with common variable Immunodeficiency/Hypogammaglobulinemia. *Front Immunol* 5: 410

Straus SK, Scott WR, Symmons MF, Marvin DA (2008) On the structures of filamentous bacteriophage Ff (fd, f1, M13). *Eur Biophys J* 37: 521−527

Swiggard WJ, Mirza A, Nussenzweig MC, Steinman RM (1995) DEC-205, a 205-kDa protein abundant on mouse dendritic cells and thymic epithelium that is detected by the monoclonal antibody NLDC-145: purification, characterization, and N-terminal amino acid sequence. *Cell Immunol* 165: 302−311

Tel J, Benitez-Ribas D, Hoosemans S, Cambi A, Adema GJ, Figdor CG, Tacken PJ, de Vries IJ (2011) DEC-205 mediates antigen uptake and presentation by both resting and activated human plasmacytoid dendritic cells. *Eur J Immunol* 41: 1014−1023

Tel J, Schreibert G, Sittig SP, Mathan TS, Buschow SI, Cruz LJ, Lambeck AJ, Figdor CG, de Vries IJ (2013) Human plasmacytoid dendritic cells efficiently cross-present exogenous Ag to CD8 + T cells despite lower antigen uptake than myeloid dendritic cell subsets. *Blood* 121: 459−467

Trapnell C, Roberts A, Goff L, Pertea G, Kim D, Kelley DR, Pimentel H, Salzberg SL, Rinn JL, Pachter L (2012) Differential gene and transcript expression analysis of RNA-seq experiments with TopHat and Cufflinks. *Nat Protoc* 7: 562−578

Trapnell C, Williams BA, Pertea G, Mortazavi A, Kwan G, van Baren MJ, Salzberg SL, Wold BJ, Pachter L (2010) Transcript assembly and quantification by RNA-Seq reveals unannotated transcripts and isoform switching during cell differentiation. *Nat Biotechnol* 28: 511−515

Trumpfheller C, Caskey M, Nchinda G, Longhi MP, Mizenina O, Huang Y, Schlesinger SJ, Colonna M, Steinman RM (2008) The microbial mimic poly IC induces durable and protective CD4 + T cell immunity together with a dendritic cell targeted vaccine. *Proc Natl Acad Sci U S A* 105: 2574−2579

Van Broekhoven CL, Parish CR, Demangel C, Britton WJ, Altin JG (2004) Targeting dendritic cells with antigen-containing liposomes: a highly effective procedure for induction of antitumor immunity and for tumor immunotherapy. *Cancer Res* 64: 4357−4365

de Verteuil DA, Rouette A, Hardy MP, Lavallée S, Trofimov A, Gaucher E, Perreault C (2014) Immunoproteasomes shape the transcriptome and regulate the function of dendritic cells. *J Immunol* 193: 1121−1132

Vicinanza M, Di Campli A, Polishchuk E, Santoro M, Di Tullio G, Godi A, Levtchenko E, De Leo MG, Polishchuk R, Sandoval L *et al* (2011) OCRL controls trafficking through early endosomes via PtdIns4,5P_2-dependent regulation of endosomal actin. *EMBO J* 30: 4970−4985

Xu J, Zoltick PW, Gamero AM, Gallucci S (2014) TLR ligands up-regulate Trex1 expression in murine conventional dendritic cells through type I Interferon and NF-κB-dependent signaling pathways. *J Leukoc Biol* 96: 93−103